A γ-ray detector with a silicon photomultiplier (SiPM) readout for neutron diffraction experiments at spallation neutron sources

2010 Meas. Sci. Technol. 21 035901

(http://iopscience.iop.org/0957-0233/21/3/035901)

Meas. Sci. Technol. **21** (2010) 035901 (6pp) doi:10.1088/0957-0233/21/3/035901

A γ-ray detector with a silicon photomultiplier (SiPM) readout for neutron diffraction experiments at spallation neutron sources

G Festa[1,5], A Pietropaolo[2], E Reali[1], F Grazzi[3] and E M Schooneveld[4]

[1] Dipartimento di Fisica, Università degli Studi di Roma Tor Vergata, Via della Ricerca Scientifica 1, 00133, Roma, Italy
[2] Dipartimento di Fisica 'G Occhialini', CNISM and Università degli Studi di Milano-Bicocca, Piazza della Scienza 3, 20126, Milano, Italy
[3] Istituto dei Sistemi Complessi—Consiglio Nazionale delle Ricerche, Via madonna del Piano 10, I-50019 Sesto Fiorentino, Firenze, Italy
[4] ISIS Facility, Rutherford Appleton Laboratory, Didcot, Oxfordshire, OX11 0QX, UK

E-mail: giulia.festa@roma2.infn.it

Received 8 October 2009, in final form 7 January 2010
Published 3 February 2010
Online at stacks.iop.org/MST/21/035901

Abstract
Standard detectors for neutron diffraction experiments are typically ^{3}He filled proportional counters. Indeed, in the near future the ^{3}He availability will be greatly reduced, so the R&D activity on alternative neutron counters is a very important issue to be addressed. Scintillator detectors could be considered as one of these alternatives. In this context, a prototype thermal neutron counter composed of a yttrium–aluminium–perovskite scintillator crystal coupled to a silicon photomultiplier (SiPM) and a standard photomultiplier tube (PMT) was used in time of flight neutron diffraction experiments on the INES spectrometer at the ISIS spallation neutron source. Neutron detection was realized by attaching the crystal to a natural cadmium sheet, used as a (n, γ) converter. Results show that the SiPM-based readout detection system has promising performances with respect to that based on a standard PMT. Diffraction patterns recorded with the ^{3}He tubes' neutron counters in use on INES allowed a comparative assessment of the SiPM-based device for time of flight neutron diffraction experiments, with respect to the standard detection technique.

Keywords: silicon photomultipliers, pulsed neutron source, neutron detectors

(Some figures in this article are in colour only in the electronic version)

Silicon photomultipliers (SiPM) are novel and very promising photosensors [1–4], made by an array of electrically decoupled pixels located on the same substrate. The operational bias voltage is higher (about 10%) than the breakdown voltage, so each pixel operates in a limited Geiger mode with a gain determined by the charge accumulated in the pixel capacitance (whose typical value is about 100 fF). In this mode, a photoelectron created in a pixel of the SiPM and reaching the high field region initiates a Geiger discharge confined to that pixel. The pixel discharge is quenched by limiting the current to about 10 μA by means of a polysilicon resistor of about 0.5 MΩ. The independently operating pixels are connected to the same readout line, so the combined output signal is the sum of all the irradiated pixels, which is a measure of the light flux impinging on the SiPM. Their main advantages as compared to standard photomultiplier tubes are insensitivity to high magnetic fields, compactness and low costs. These

[5] Author to whom any correspondence should be addressed.

devices have been used mostly in particle physics, e.g. together with the front-end electronics developed for the compact muon solenoid hadron calorimeter (CMS HCAL) [5], or in the experimental search for supersymmetric neutral particles with liquid xenon scintillators [6]. These devices have also been tested for Ring Imaging Cherenkov (RICH) detectors [6] and then used in experimental measurements, in a proximity focusing RICH with an aerogel radiator, for the Belle detector at the KEK B-factory [7, 8]. Recent technology SiPM devices have been extensively investigated by Finocchiaro *et al* who also provided a thorough and reliable characterization protocol for these photosensors [9, 10]

Neutron applications of SiPM are worth closely investigating as well, for example at pulsed neutron sources. Very recently a time of flight (TOF) neutron spectroscopy application [11] has been identified in neutron resonance capture analysis (NRCA) experiments carried out on the INES beam line [12–14] at the ISIS spallation neutron source (UK) [15].

The main issue of the present study is the assessment of the potential of a detection device composed of a yttrium–aluminum–perovskite (YAP) scintillator crystal, a SiPM readout and a (n, γ) cadmium foil converter, for neutron diffraction measurements at spallation sources. Neutron diffraction measurements on INES are typically performed using the array of ^{3}He tubes at 20 bar pressure at disposal. While in the case of the YAP–SiPM device neutron counting proceeds by detecting the radiative neutron capture gamma in Cd, for the helium counters this is accomplished by the detection of the secondary charged particles (alpha and tritium) generated upon neutron absorption on ^{3}He. The main advantage of the former system relies in the possibility of obtaining an almost constant neutron detection efficiency in an extended neutron energy range, while the ^{3}He counters suffer E^{-05} detection efficiency loss. Furthermore, being fast devices, the scintillators could support higher rates as compared to pressurized gaseous detectors. Moreover, it is well known that in the near future ^{3}He availability will be greatly reduced; therefore, different solutions for thermal neutron detection are worth exploring. To this aim, a prototype YAP–Cd–SiPM detector, mentioned above, was designed, produced and then tested on the INES diffractometer.

1. Experimental details

Neutron diffraction (ND) is a powerful technique for investigating the crystal structure of materials [16, 17].

The diffraction process is described as the reflection of the incident beam by crystal planes $[hkl]$. The well-known Bragg's law $\lambda = \frac{d_{hkl}\sin(\vartheta)}{n}$ links together d_{hkl} (the spacing relative to a set of lattice planes), the scattering angle $2\vartheta_0$ and the wavelength λ of the incident radiation. In order to obtain a full diffraction pattern from a powder sample, one of the two parameters $2\vartheta_0$ or λ can be varied leaving the other constant. Standard monochromatic diffraction exploits the different scattering angle related to different d_{hkl} plane distances by Bragg's law with constant λ. Diffractometers operating at a spallation source are instead based on the determination of neutron energy (thus wavelength), through the TOF technique, i.e.

$$E = \frac{1}{2}m_n v^2 = \frac{1}{2}m_n\left(\frac{L}{t}\right)^2 \tag{1}$$

where m_n is the mass of the neutron, v is its velocity, L is the total flight path (from the moderator to the detector) and t is the time of flight. Using the de Broglie relation, equation (1) becomes

$$E = \frac{1}{2}m_n\left(\frac{h}{m_n\lambda}\right)^2, \tag{2}$$

h and λ being Planck's constant and the neutron's wavelength, respectively.

It is hence possible to rewrite the relationship between λ and the time of flight:

$$\lambda = \frac{ht}{m_n L}, \tag{3}$$

and Bragg's law can be rewritten in terms of TOF (t_{hkl}) as

$$t_{hkl} = \frac{2m_n}{h}Ld_{hkl}\sin(\vartheta_0) \tag{4}$$

where $2\vartheta_0$ is a (fixed) scattering angle and d_{hkl} is the spacing relative to a set of lattice planes.

The experimental signal from a TOF diffraction measurement is a pattern of Bragg peaks. The peaks' positions are directly related to the crystal lattice dimensions and are used to identify phases, structures and/or to infer texture information through line-shape analysis [18, 19]. The last kind of analysis is still a semi-quantitative technique but it can infer useful information on thermal and mechanical treatments and the grain size of the sample [20].

In order to test the detection device, a neutron diffraction experiment on a Fe slab was carried out; a schematic layout of the setup is shown in figure 1. The total flight path was $L \approx 23$ m. The YAP–SiPM–PMT system (figure 2) was placed at a scattering angle $2\vartheta \approx 85^\circ$ and was connected to the same data acquisition electronics (DAE) as the ^{3}He tubes, routinely employed on INES for neutron diffraction experiments. This allowed a comparison between SiPM and PMT not only for thermal neutron counting, but also with the standard neutron counters.

The YAP crystal utilized for the tests was manufactured by Crytur [21] and its dimensions were 6 mm × 6 mm × 25 mm, with a decay constant of 27 ns and a wavelength of maximum emission $\lambda_m = 350$ nm. In order to make the YAP sensitive to thermal neutrons, it was attached to a natural cadmium sheet of 50 μm thickness and about 1 cm^2 surface area. The SiPM and PMT were both from Hamamatsu [22]; the active area of the SiPM was 1 mm^2 (1600 pixels) and the surface area of the photocathode of the PMT was about 50 mm^2. For the measurements, the YAP crystal was used without any reflecting or diffusive material. The ^{3}He tubes, manufactured by EURISYS (now Canberra Eurisys), were 100 mm in height, 12.5 mm in diameter and 2.5 mm in thickness at a pressure $p = 20$ bar, providing a detection efficiency of about 50% at $E_n = 25$ meV, decreasing as ${E_n}^{-0.5}$ [23].

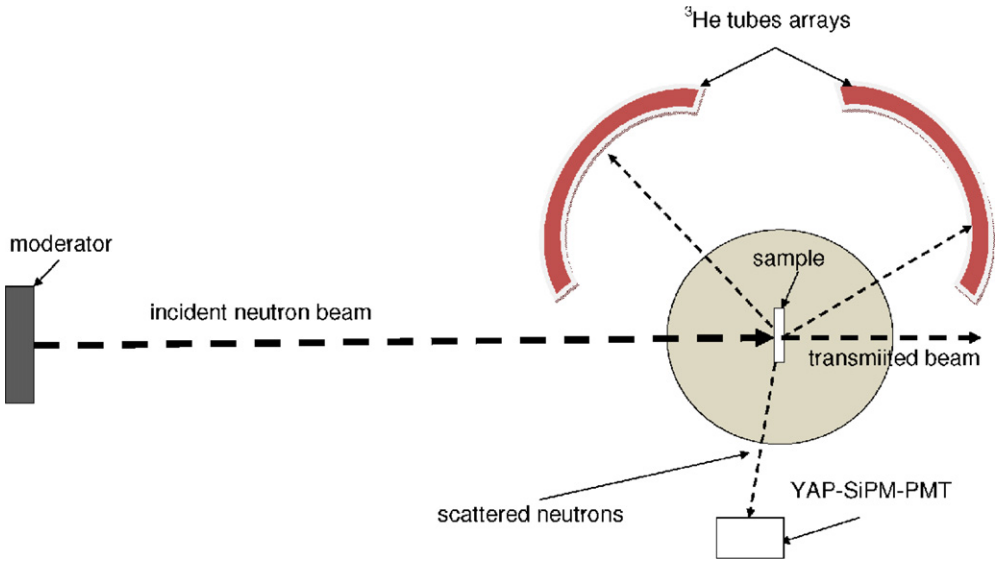

Figure 1. Schematic layout of the diffraction experiment at the INES diffractometer.

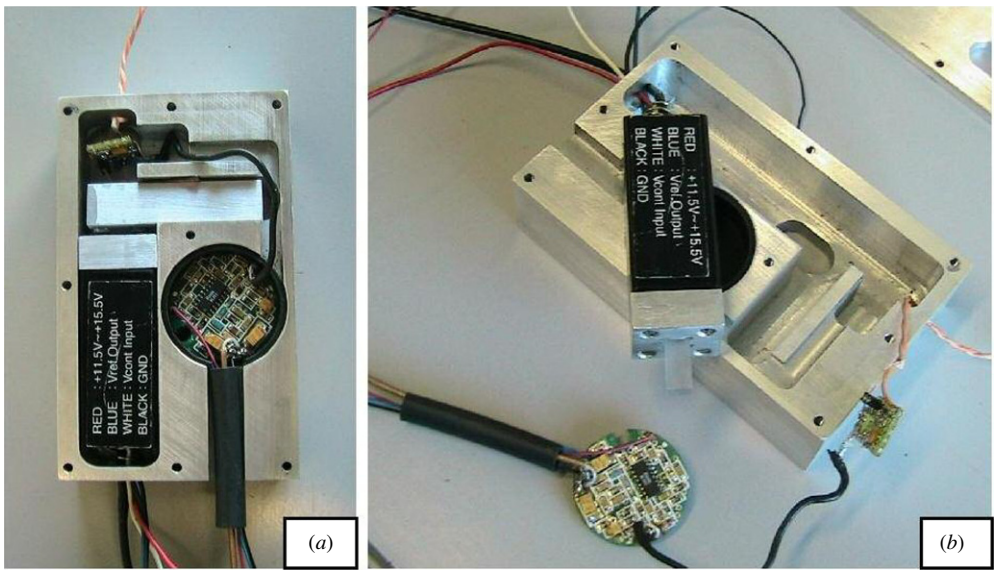

Figure 2. Pictures of the detection system YAP–SiPM–PMT. Part of the front end electronics is also visible.

The employment of Cd allows us to build a neutron counter based on the radiative capture of thermal neutrons in this material. Indeed the thermal neutron radiative capture cross section $\sigma_{\mathrm{RC}}(E)$ is very wide up to the so-called cadmium cut-off, as shown in figure 3, where the $\sigma_{\mathrm{RC}}(E)$ of natural Cd is plotted up to 500 meV [24]. When a neutron is absorbed in the Cd, a prompt γ-ray cascade is generated within 10^{-9}–10^{-12} s. It is composed of several lines, the strongest transitions (relative intensity $I_r = 100\%$) being at energy E_γ = 245.30 keV (^{110}Cd), E_γ = 617.52 keV (^{111}Cd), E_γ = 558.5 keV (^{113}Cd). The signals were sent to a timing filter amplifier and to a discriminator before being processed by the DAE. The lower level discrimination (LLD) threshold was set at about 300 keV (energy equivalent) for the PMT. The LLD for the SiPM was set at a value corresponding to about 5 pixels threshold, thus providing an appreciable reduction of the intrinsic (thermally activated) noise. This threshold was higher with respect to the one set for the PMT, resulting in a lower counting rate. The acquisition time frame was 20 ms wide and started with the ISIS trigger, provided by the proton pulse, with a repetition rate of 50 Hz. The multi-stops were provided by the neutron counters upon absorption of the scattered neutrons. In the case of the ^{3}He tubes, neutron counting was provided by the detection of the secondary charged particles produced in the reaction: n + ^{3}He $\rightarrow$ p + t + Q, p being the proton, t the tritium and Q the (positive) Q-value that, for this reaction, is 0.764 MeV. In the case of the YAP–SiPM and YAP–PMT the stops were provided by the detection of the light flashes of the scintillator following neutron absorption in the Cd converter foil.

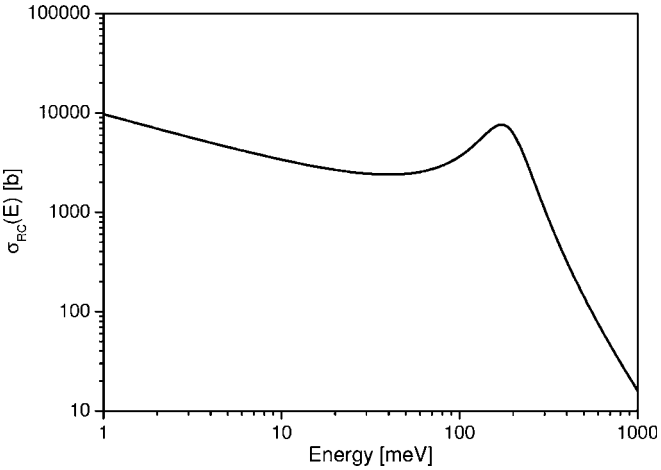

Figure 3. Radiative capture cross section $\sigma_{RC}(E)$ for natural cadmium.

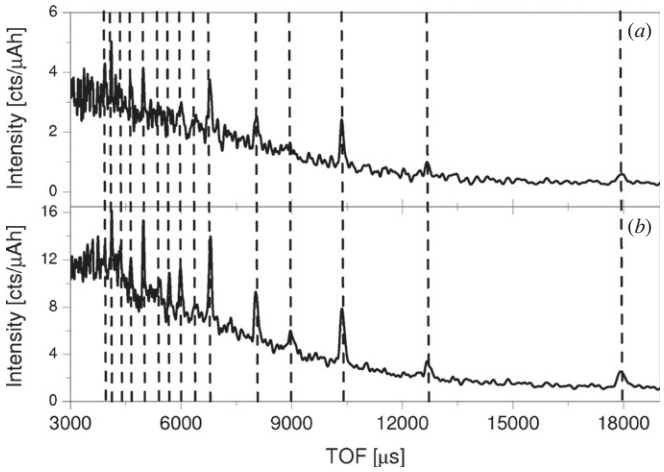

Figure 4. Neutron TOF spectra recorded by SiPM (*a*) and PMT (*b*) during a Fe slab sample irradiation. Total time data recorded is the same for the two detectors.

2. Results and discussion

Figure 4 shows the typical TOF diffraction pattern registered by the YAP–SiPM and YAP–PMT systems during the same acquisition time (corresponding to a total integrated current $I = 2586\ \mu$A h).

The two spectra show the same peak positions and a similar trend of the continuum beneath the peaks. The spectra have indeed different intensities, the PMT's spectrum being on average higher with respect to the SiPM one. This is clear from figure 5, where the ratio of the two spectra is shown in the same TOF region as of figure 4. It can be noted that the ratio is almost constant over the whole TOF region, with a mean value of about 3.65.

Figure 6 shows the TOF diffraction pattern recorded by a ^{3}He tube at the same scattering angle as the YAP crystal. The diffraction peaks appear at the same time positions as for the other two spectra. The ^{3}He spectrum is much more intense compared to the others and this is mostly due to geometrical effects. Indeed the He-tubes have a geometrical acceptance higher by a factor of 15 as compared to the Cd sheet that is

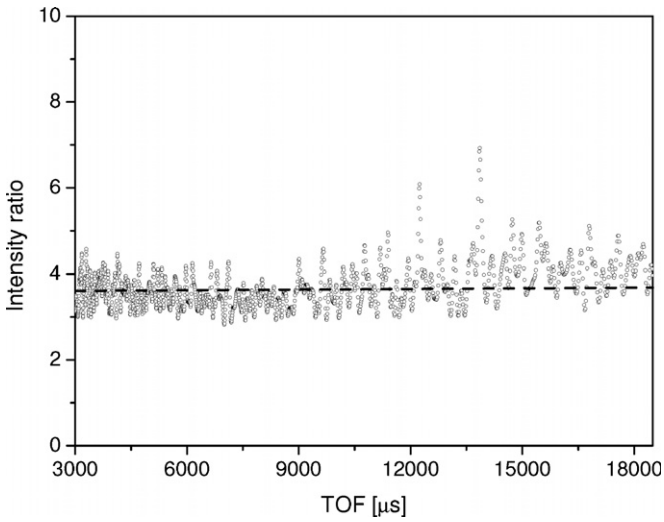

Figure 5. Intensity ratio of the two spectra shown in the same TOF region as in figure 4. The ratio is almost constant with a mean value of about 3.6.

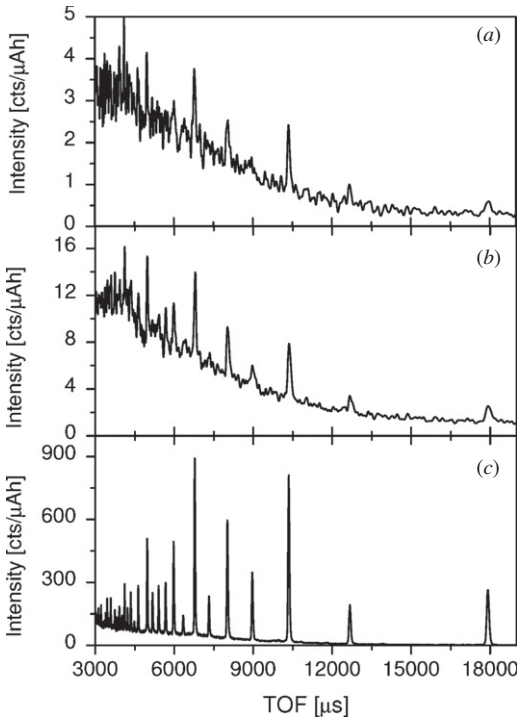

Figure 6. Neutron TOF spectra from a Fe sample recorded by the YAP–SiPM, YAP–PMT and ^{3}He tube. Total time data recording is the same for the three detectors.

a neutron-sensitive material. Considering that the Cd sheet was not in contact with the YAP, but was at a distance of about 3 mm, and that the radiative capture γ-rays' emission is isotropic, the fraction of the solid angle subtended by the crystal is lower than 0.5. Thus an overall factor of at least 30 has to be considered for the overall relative geometrical acceptance between the two devices.

The peak positions recorded by the three detectors (^{3}He, PMT, SiPM) are listed in table 1; it can be noted that their positions are almost the same. To allow for a comparison of

Table 1. Time of flight diffraction peaks position recorded by the three detectors, namely ^{3}He, YAP–PMT and YAP–SiPM.

TOF ^{3}He (μs)	TOF PMT (μs)	TOF SiPM (μs)
17 927 ± 18	17 938 ± 18	17 949 ± 18
12 680 ± 13	12 691 ± 13	12 680 ± 13
10 355 ± 11	10 366 ± 11	10 360 ± 11
8967 ± 10	8966 ± 10	8961 ± 10
8017 ± 8	8023 ± 8	8040 ± 8
7314 ± 7	7257 ± 7	7190 ± 7
6783 ± 7	6783 ± 7	6778 ± 7
6331 ± 7	6383 ± 7	6400 ± 7
5966 ± 6	5977 ± 6	6501 ± 6
5669 ± 5	5669 ± 5	5664 ± 5
5406 ± 5	5383 ± 5	5371 ± 5
5177 ± 5	5171 ± 5	5164 ± 5
4998 ± 5	4994 ± 5	4966 ± 5
4623 ± 4	4629 ± 4	4617 ± 4
4355 ± 4	4327 ± 4	4320 ± 4
4104 ± 4	4103 ± 4	4103 ± 4

Table 2. Characteristics of time of flight diffraction peaks recorded by the three detectors: (a) ^{3}He, (b) YAP–PMT and (c) YAP–SiPM. The second and the third columns report maximum value of counts for the single peak and background. Signal was calculated by P − B, and S/B is the signal to background ratio.

TOF (μs)	Peak (P)	Background (B)	Signal (S)	S/B
		(a) ^{3}He detector		
4998	512	72	440	6.11
6783	896	59	837	14.19
10 355	812	22	790	35.91
17 926	266	11	255	23.18
		(b) Cd foil: YAP–PMT		
4998	15.0	8	7.0	0.87
6783	14.0	6	8.0	1.33
10 355	8.0	3	5.0	1.67
17 926	2.5	1	1.5	1.50
		(c) Cd foil: YAP–SiPM		
4998	4.2	2.3	1.9	0.8
6783	3.8	1.7	2.1	1.2
10 355	2.4	0.8	1.6	2.0
17 926	0.6	0.1	0.5	5.0

the devices, the main characteristics of time of flight diffraction peaks recorded by the three detectors were analysed especially in terms of signal and background intensities (see table 2). The signal at the peak positions is on average two orders of magnitude higher for the He tube as compared to the YAP device. Also the signal to background ratio is higher. This is due to the lower sensitivity of the He tube to environmental γ-rays and to a not completely optimized LLD threshold for the PMT [25] and SiPM.

It has to be stressed that the count rate can be improved by an order of magnitude by enhancing the geometrical acceptance (a bigger crystal and Cd sheet, at least matching the He tube size). As shown in figure 7, a thicker Cd sheet (e.g. 100 μm) slightly enhances the neutron absorption probability, whereas the shielding effect on the radiative capture γ-ray is still negligible. The use of a reflecting material around the YAP (e.g. mylar) may enhance the light flux onto the SiPM/PMT. This could allow the LLD to be set at about 500–600 keV cutting out the appreciable contribution of the

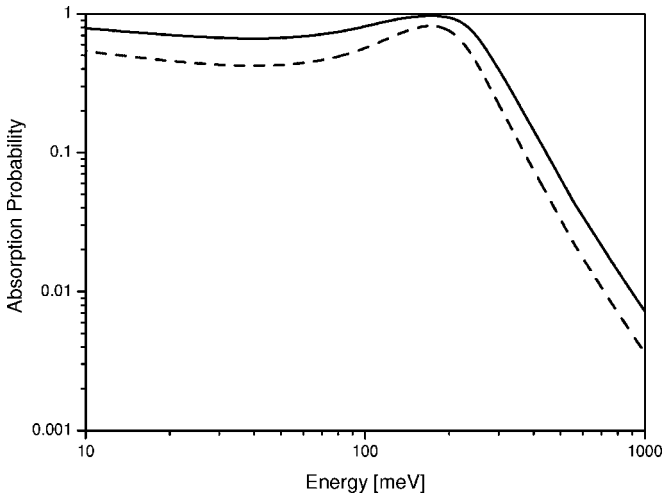

Figure 7. Neutron absorption probability $T(E)$ for two Cd sheets of 50 μm (dashed line) and 100 μm (continuous line) thickness.

480 keV radiative capture γ-rays from n–^{10}B reactions (neutron absorption in the walls of the instrument hall) [25]. On average, a similar counting efficiency and S/B should be expected for SIPM and PMT. Despite the performance of the He tube not being reached by the YAP-based counter, the performance of the latter device may be greatly improved also for a reliable line-shape analysis. Indeed line-shape analysis on scattering peaks is already carried out in inelastic neutron scattering measurements at ISIS employing γ-ray detectors in the epithermal energy range [26, 27].

3. Conclusions

The results obtained show the effectiveness and the potential of the SiPM technology for neutron diffraction measurements at spallation sources with γ-ray detectors. Unlike the ^{3}He gas tubes, a neutron counter based on the radiative capture γ-rays detection does not suffer $E^{-0.5}$ detection efficiency loss. Last but not the least, ^{3}He availability will be greatly reduced in the near future and thus the R&D on new neutron counters based on different approaches is worth carrying out.

As a final remark, it has to be stated that the new-generation spallation neutron sources (e.g. SNS) will provide higher neutron fluxes as compared to those available at present (e.g. on TS1 at ISIS). At these high flux neutron sources, rate capability is an issue to be addressed and fast scintillators, such as the one investigated in this paper, could fulfil this requirement.

Despite the performance of standard He tube neutron counter being better than the YAP-based neutron counter, possible improvements of the latter device may be considered to enhance counting efficiency and S/B. An optimized counter based on radiative capture γ-rays with a SiPM readout may have at least comparable overall performance to the He tubes presented in this paper. Further tests on an upgraded device are foreseen and new results are expected in the new experimental campaign that will be carried out at ISIS in the near future.

Acknowledgments

This work was supported within the CNR-CCLRC agreement no 01/9001 concerning collaboration in scientific research at the spallation neutron source ISIS. The financial support of the Consiglio Nazionale delle Ricerche in this research is hereby acknowledged.

References

[1] Bondarenko G, Dolgoshein B, Golovin V, Ilyin A, Klanner R and Popova E 1998 *Nucl. Phys.* B **61** 347
[2] Bondarenko G *et al* 2000 *Nucl. Instrum. Methods* A **442** 187
[3] Buzhan P *et al* 2002 The advanced study of silicon photomultiplier *Proc. 7th Int. Conf. on Advance Technology & Particle Physics* p 717
[4] Buzhan F P *et al* 2003 *Nucl. Instrum. Methods* A **504** 48
Dolgoshein B *et al* 2006 *Nucl. Instrum. Methods* A **563** 368
Renker D 2006 *Nucl. Instrum. Methods* A **567** 48
[5] Britvitch I, Musienko Y and Renker D 2006 *Nucl. Instrum. Methods* **557** 276
[6] Aprile E, Cushman P, Ni K and Shagin P 2006 *Nucl. Instrum. Methods* **556** 215
[7] Korpar S, Dolenec R, Hara K, Iijima T, Krizan P, Mazuka Y, Pestotnik R, Stanovnik A and Yamaoka M 2008 *Nucl. Instrum. Methods* A **595** 161
[8] Čerenkov P A 1937 *Phys. Rev.* **52** 378
[9] Finocchiaro P *et al* 2008 *IEEE Trans. Electron Devices* **55** 2757
[10] Finocchiaro P *et al* 2008 *IEEE Trans. Electron Devices* **55** 2765
Finocchiaro P, Pappalardo A, Cosentino L, Belluso M, Billotta S, Bonanno G and Di Mauro S 2008 *IEEE Trans. Electron Devices* **55**
[11] Pietropaolo A, Gorini G, Festa G, Andreani C, De Pascale M P, Reali E, Grazzi F and Schooneveld E M 2009 *Rev. Sci. Instrum.* **80** 9
[12] Notiziario CNR 2006 *Neutroni e Luce di Sincrotrone* **11** 6
[13] Imberti S *et al* 2008 *Meas. Sci. Technol.* **19** 034003
[14] Celli M, Grazzi F and Zoppi M 2006 *Nucl. Instrum. Methods* A **565** 861
[15] ISIS web site: http://www.isis.rl.ac.uk
[16] Squires G L 1978 *Introduction to the Theory of Thermal Neutron Scattering* (Mineola, NY: Dover)
[17] Lovesey S W 1984 *Theory of Neutron Scattering from Condensed Matter* vol 1 (Oxford: Oxford University Press)
[18] Arletti R, Cartechini L, Rinaldi R, Giovannini S, Kockelmann W and Cardarelli A 2008 *Appl. Phys.* A **90** 9
[19] Siano S, Kockelmann W, Bafile U, Celli M, Iozzo M, Miccio M, Moze O, Pini R, Salimbeni R and Zoppi M 2002 *Appl. Phys.* A **74** S1139
[20] Siano S, Bartoli L, Zoppi M, Kockelmann W, Daymond M, Dann J A, Garagnani M G and Miccio M 2003 *Proc. Archaeometallurgy in Europe* vol 2 p 319
[21] crytur web site: http://www.crytur.cz/
[22] Hamamatsu web site: http://www.hamamatsu.com/
[23] Canberra website: http://www.canberra.com/
[24] kaeri web site: http://atom.kaeri.re.kr
[25] Tardocchi M, Gorini G, Pietropaolo A, Andreani C, Senesi R, Rhodes N and Schooneveld E M 2004 *Rev. Sci. Instrum.* **75** 4880
[26] Pietropaolo A, Andreani C, Filabozzi A, Senesi R, Gorini G, Perelli Cippo E, Tardocchi M, Rhodes N J and Schooneveld E M 2006 *J. Instrum.* **1** P04001
[27] Pietropaolo A, Andreani C, Senesi R, Botti A, Bruni F and Ricci M A 2008 *Phys. Rev. Lett.* **100** 127802